The Mean Along-Isobath Heat and Salt Balances over the Middle Atlantic Bight Continental Shelf

STEVEN J. LENTZ

Woods Hole Oceanographic Institution, Woods Hole, Massachusetts

ABSTRACT

The mean heat and salt balances over the Middle Atlantic Bight continental shelf are investigated by testing the hypothesis that surface fluxes of heat or freshwater are balanced by along-isobath fluxes resulting from the mean, depth-averaged, along-isobath flow acting on the mean, depth-averaged, along-isobath temperature or salinity gradient. This hypothesized balance is equivalent in a Lagrangian frame to a column of water, for example, warming because of surface heating as it is advected southward along isobath by the mean flow.

Mean depth-averaged temperatures increase from north to south along isobath at a rate of $2°C\,(1000\ km)^{-1}$ at midshelf, which is consistent with the hypothesized balance and mean surface heat flux estimates from the 50-yr NCEP Reanalysis. However, mean surface heat flux estimates from the higher-resolution 20-yr Objectively Analyzed Air–Sea Fluxes (OAFlux) reanalysis are too small to balance the along-isobath heat flux divergence implying a cross-shelf heat flux convergence. It is unclear which surface heat flux estimate, NCEP or OAFlux, is more accurate. The cross-shelf heat flux convergence resulting from the mean cross-shelf circulation is too small to balance the along-isobath heat flux divergence.

Mean depth-averaged salinities increase from north to south along isobath at a rate of $1\,(psu)\,(1000\ km)^{-1}$ at midshelf. Mean precipitation and evaporation rates nearly balance so that the net freshwater flux is too small by more than an order of magnitude to account for the observed along-isobath increase in salinity. The cross-shelf salt flux divergence resulting from the mean cross-shelf circulation has the wrong sign to balance the divergence in the along-isobath salt flux. These results imply there must be an onshore "eddy" salt flux resulting from the time-dependent current and salinity variability.

The along-isobath temperature and salinity gradients compensate for each other so that the mean, depth-averaged, along-isobath density gradient is approximately zero. This suggests that there may be a feedback between the along-isobath density gradient and the onshore salt and heat fluxes that maintains the density gradient near zero.

1. Introduction

The Middle Atlantic Bight (MAB) continental shelf waters between Cape Hatteras (CH) to the south and Georges Bank (GB) to the north (Fig. 1) are on average cooler and less salty than the adjacent waters over the continental slope (e.g., Bigelow 1933; Bigelow and Sears 1935; Loder et al. 1998). A persistent shelf–slope front separates the distinct shelf and slope waters (Linder and Gawarkiewicz 1998). Shelf waters are warm in summer (20°C near the surface) and cold (5°C) in winter (e.g., Bigelow 1933; Mayer et al. 1979; Beardsley and Boicourt 1981; Beardsley et al. 1985; Butman and Beardsley

1987). This seasonal variation in water temperature is primarily caused by a seasonal variation in surface heat flux with solar heating warming the ocean in spring–summer and latent and sensible heat loss cooling the ocean in fall–winter (e.g., Austin and Lentz 1999; Flagg et al. 2002; Bignami and Hopkins 2003; Lentz et al. 2003a; Lentz 2003; Fewings et al. 2008; Lentz et al. 2010, manuscript submitted to *J. Geophys. Res.,* hereafter LSP). The mean (time scales long compared to a year) surface heat flux over the MAB is positive (heat fluxes into the ocean) with a magnitude of about $10\ W\ m^{-2}$ (Beardsley and Boicourt 1981; Joyce 1987). In the absence of advective fluxes, this implies a depth-averaged temperature increase of approximately $1°C\ yr^{-1}$ in 100 m of water (maximum water depth of the continental shelf) and larger increases in shallower water. This is 100 times larger than the observed temperature increase of 1°–2°C

Corresponding author address: Steven J. Lentz, Woods Hole Oceanographic Institution, MS 21, Woods Hole, MA 02543.
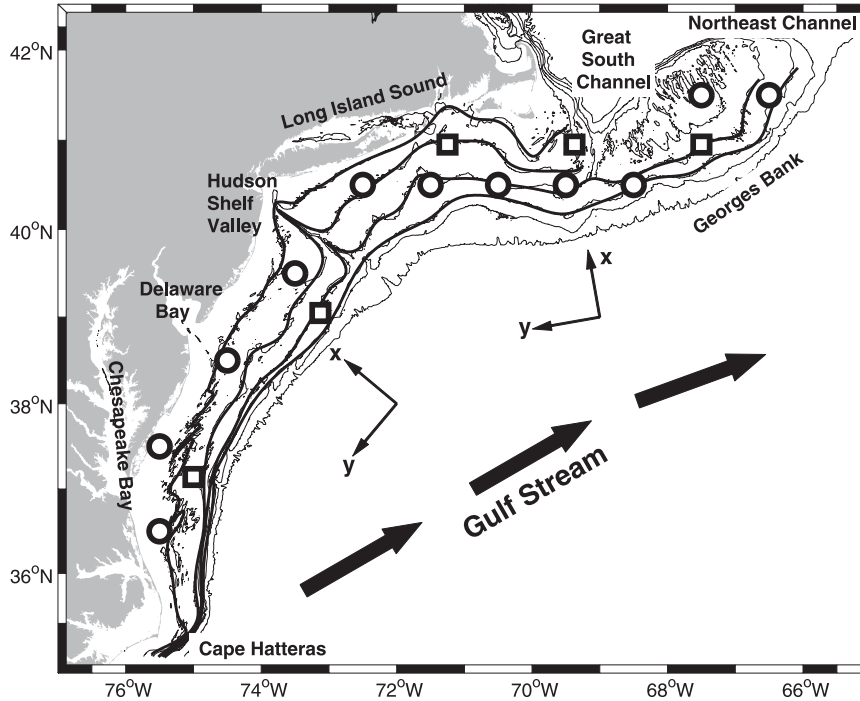E-mail: slentz@whoi.edu

FIG. 1. Map of the MAB showing bathymetry and locations of centers of NCEP reanalysis (squares; $\approx 2°$ squares) and OAFlux (circles; 1°) latitude–longitude grid cells used to estimated surface flux. The 30-, 50-, 70-, 90-, 120-, and 1000-m isobaths (thin lines) and the smoothed 30-, 50-, 70-, and 90-m isobaths (thick lines) used in the analysis are shown. The mean location of the Gulf Stream is also shown (Joyce et al. 2000).

over the last 100 yr (Stearns 1965; Maul et al. 2001; Nixon et al. 2004; Shearman and Lentz 2010). This discrepancy implies that the mean surface heat flux into the MAB shelf water is removed by some advective process. One objective of this study is to determine what balances the mean surface heat flux.

As a first step toward a quantitative understanding of the mean heat balance for the MAB, the simple hypothesis is tested that the mean surface heat flux is balanced by an along-isobath advection of cooler water from the north. The mean flow in the MAB is along isobath toward the south and west at ≈ 0.1 m s^{-1} (Bumpus 1973; Beardsley et al. 1976; Beardsley and Boicourt 1981; Lentz 2008). In a Lagrangian frame, a column of water starting at Georges Bank warms because of surface heating as it flows southward along an isobath, resulting in an along-isobath temperature gradient. The corresponding Eulerian mean heat balance is

$$\hat{v}h\hat{T}_y = \frac{Q}{\rho_o C_p}, \qquad (1)$$

where $\hat{v}$ is the mean depth-averaged along-isobath current, h is the water depth, $\hat{T}_y$ is the mean depth-averaged

along-isobath temperature gradient, Q is the mean surface heat flux, $\rho_o = 1025$ kg m^{-3} is a representative seawater density, and $C_p = 4190$ W (kg °C)$^{-1}$ is the heat capacity of seawater. The along-isobath temperature gradient is therefore

$$\hat{T}_y = \frac{Q}{\rho_o C_p h \hat{v}}. \qquad (2)$$

Recently, LSP found that (1) was the approximate mean heat balance on the New England shelf during a 10-month moored array deployment in 1996–97.

The MAB salt balance has received less attention than the heat balance, in part because of the difficulty of making accurate moored salinity measurements (e.g., Bignami and Hopkins 2003; LSP). In contrast to temperature, salinity does not exhibit a large seasonal variation (Bigelow and Sears 1935; Manning 1991). Mean net freshwater surface flux (precipitation minus evaporation) over the MAB is small relative to both freshwater runoff within the MAB and the along-shelf freshwater flux from the north (Beardsley and Boicourt 1981; Joyce 1987; Mountain 2003). The along-isobath salt balance corresponding to (1) is

$$\hat{v}h\hat{S}_y = -(P - E)S_{\mathrm{o}}, \qquad (3)$$

where S is salinity, P is the mean precipitation rate, E is the mean evaporation rate, and $S_{\mathrm{o}} = 32$ is a reference salinity (salinity values are based on the practical salinity scale). Using a constant reference salinity on the right-hand side of (3) is an accurate approximation because $\hat{v}h/(P - E)$ is large compared to the along-isobath length scale of the MAB.

The hypothesized balances, (1) and (3), intentionally neglect a number of potentially important contributions to the heat and salt balances, notably cross-shelf fluxes resulting from wind forcing, instabilities, warm-core rings, and other processes (e.g., Wright 1976; Csanady and Magnell 1987; Loder et al. 1998; Brink 1998). The degree to which the mean surface heat flux and along-isobath heat flux divergence balance or do not balance provides insight into the importance of these other processes.

The hypothesized heat and salt balances are tested using historical ship observations to characterize the depth-averaged along-isobath temperature and salinity gradients and historical meteorological reanalysis estimates of the surface heat and freshwater fluxes. These observations indicate that there are mean along-isobath temperature and salinity gradients over the MAB shelf that result in substantial along-isobath heat and salt flux divergences. The along-isobath heat flux divergence over the shelf may be either partially or entirely balanced by surface heating depending on the reanalysis estimate used in the analysis. Evaporation minus precipitation is too small to balance the along-isobath salt flux divergence, which implies that there is a substantial cross-shelf (on-shore) salt flux over the MAB shelf.

2. Heat and salt balances

A coordinate system is used with y along-isobath positive equatorward (direction of mean flow), x positive onshore, and z positive upward. The steady, depth-averaged heat balance is

$$\frac{\partial}{\partial x}\int_{-h}^{0}\overline{uT}\,dz + \frac{\partial}{\partial y}\int_{-h}^{0}\overline{vT}\,dz = \frac{Q}{\rho_{\mathrm{o}}C_p}, \qquad (4)$$

where u and v are the cross- and along-isobath velocities, T is temperature, and an overbar indicates a time average. The flux through the seafloor is assumed to be negligible; for simplicity, sea surface height variations are assumed small compared to h and neglected. For the time scales of interest here, years, the time rate of change in temperature is small compared to the surface heat flux.

Each variable is decomposed into its time-averaged and fluctuating components: for example, $T(x, y, z, t) =$

$\overline{T}(x, y, z) + T'(x, y, z, t)$. Time averages are further decomposed into depth-averaged and depth-dependent components: for example, $\overline{T}(x, y, z) = \hat{T}(x, y) + \tilde{T}(x, y, z)$. The resulting heat balance is

$$\hat{v}h\frac{\partial \hat{T}}{\partial y} + \frac{\partial}{\partial x}\int_{-h}^{0}\tilde{u}\tilde{T}\,dz + \frac{\partial}{\partial y}\int_{-h}^{0}\tilde{v}\tilde{T}\,dz$$

$$+ \frac{\partial}{\partial x}\int_{-h}^{0}\overline{u'T'}\,dz + \frac{\partial}{\partial y}\int_{-h}^{0}\overline{v'T'}\,dz = \frac{Q}{\rho_{\mathrm{o}}C_p}, \qquad (5)$$

where terms that depend on $\partial\hat{v}/\partial y$ and $\hat{u}$ are assumed small based on mean current observations (Lentz 2008).

The corresponding salt balance is

$$\hat{v}h\frac{\partial \hat{S}}{\partial y} + \frac{\partial}{\partial x}\int_{-h}^{0}\tilde{u}\tilde{S}\,dz + \frac{\partial}{\partial y}\int_{-h}^{0}\tilde{v}\tilde{S}\,dz + \frac{\partial}{\partial x}\int_{-h}^{0}\overline{u'S'}\,dz$$

$$+ \frac{\partial}{\partial y}\int_{-h}^{0}\overline{v'S'}\,dz = -(P - E)S_{\mathrm{o}}. \qquad (6)$$

The focus here is on the extent to which surface fluxes (terms on right-hand side) are balanced by the mean along-isobath flow acting on the mean along-isobath temperature or salinity gradient (first terms on left-hand side): that is, (1) and (3). The discrepancy between these two terms provides insight into the size of the other terms in (5) and (6), notably the cross-isobath fluxes of heat and salt. The size of the heat and salt flux divergence resulting from the mean, depth-dependent cross-isobath flow [second terms on the left-hand sides of (5) and (6)] are also estimated (sections 5a and 5b and appendix).

3. Data and processing

The analysis focuses on determining the along-isobath distribution of the mean depth-averaged temperature and salinity using historical hydrographic data (section 3c) and comparing that distribution to the surface heat and freshwater fluxes (section 3d) in the context of (1) and (3).

a. Bathymetry

The analysis is carried out along the 30-, 50-, 70-, and 90-m isobaths using the National Geophysical Data Center (NGDC) high-resolution continental shelf bathymetry (Fig. 1). The 70- and 90-m isobaths start at the northeast corner of Georges Bank and extend to Cape Hatteras. The 30- and 50-m isobaths used here start west of Great South Channel (GSC) between Cape Cod and Georges Bank, because these isobaths are not connected to the southern flank of Georges Bank. The isobaths were smoothed to reduce variability on spatial scales less than about 20 km, notably because of ridge and

swale features along the 30-m isobath (Fig. 1). The 90-m isobath is near the shelf break throughout the MAB. The 50- and 70-m isobaths are at roughly midshelf over Georges Bank and the New England shelf but at or near the shelf break in the southern MAB. This change in the isobath positions relative to the shelf break complicates interpretation of the observations because there are changes in the along-isobath temperature or salinity that are associated with proximity to the warmer, saltier slope water. Additionally, there are fewer profiles for isobaths near the shelf break, because the isobaths are closer together as a result of the steeper bottom slope.

b. Along-isobath mean flow

The mean depth-averaged flow in the Middle Atlantic Bight is equatorward, along isobath, and increases with increasing water depth (Beardsley and Boicourt 1981; Lentz 2008). Based on analysis of moored current time series longer than 200 days from 33 sites in the MAB, Lentz (2008) found empirically that the depth-averaged, along-isobath velocity (m s^{-1}) is to a good approximation

$$\hat{v} \approx 0.02 + 0.0007h, \qquad (7)$$

where h is total water depth in meters. This expression is used to estimate $\hat{v}$ along each isobath. Lentz (2008) found that, for the limited set of long current time series, both interannual variability and along-isobath variations in $\hat{v}$ are small (≈ 0.01 m s^{-1} or less) and that the depth-averaged cross-shelf velocities $\hat{u}$ are small.

c. Temperature and salinity observations

Temperature and salinity profiles from the National Oceanographic Data Center's World Ocean Database 2001 archive of ship observations are analyzed. Water depths for each profile were determined from the latitude and longitude of the profile and the NGDC bathymetry of the MAB continental shelf. Only profiles were included with at least $h/10 + 1$ samples in the vertical and at least 1 sample within 5 m of the surface and 15 m of the bottom. Profiles in Chesapeake Bay (CB), Delaware Bay (DB), and Long Island Sound (LIS) were excluded from the analysis. The resulting dataset consists of 39 155 temperature profiles, 10 581 salinity profiles, and 8830 density profiles between the 20- and 100-m isobaths. The profiles span the period 1913–2000, but the distribution is heavily weighted to recent times. Half the temperature profiles were collected after 1968, and half the salinity profiles were collected after 1986. The annual distribution of sampling is not uniform, with 18% of the samples in winter (December–February), 34% in spring (March–May), 25% in summer (June–August), and 23% in autumn (September–November).

Depth averages were computed using trapezoidal integration and assuming temperature, salinity, or density was uniform between the measurement nearest the surface (bottom) and the surface (bottom). To estimate mean distributions along the 30-, 50-, 70-, and 90-m isobaths, all depth-averaged values were found for a band of water depths within ±10 m of the given isobath: for example, between the 60- and 80-m isobaths for the 70-m isobath distribution (Fig. 1). There is a large annual cycle in temperature and hence density over the MAB shelf (Bigelow 1933; Beardsley and Boicourt 1981). Therefore, to reduce aliasing the means by the uneven sampling of the annual cycle noted earlier, a mean and an annual cycle were fit to all the depth-averaged temperatures, salinities, or densities in a given isobath range in each of three regions: Georges Bank, the New England shelf, and the MAB shelf south of Hudson Shelf Valley (HSV). The annual cycle for each region and isobath range was then subtracted from each observation. Including a semiannual cycle in the fits did not change the results. The depth-averaged temperature, salinity, or density anomalies for a given isobath were then bin averaged in 100-km along-isobath intervals to estimate the along-isobath variation of the mean temperature, salinity, or density. Temperature, salinity, and density time series from moorings indicate these variables have a decorrelation time scale of about 10 days (with the annual cycle removed). Therefore, samples in an along-isobath bin within 10 days of each other were averaged to form one value so that each bin sample is independent. Uncertainties in the bin averages, indicated as 95% confidence intervals (CIs), were determined using the standard error of the mean, $1.96\sigma/\sqrt{n}$, where σ is the standard deviation and n is the number of independent samples in the bin average. The choices of ±10-m isobath bin width and 100-km along-isobath bin length were a compromise between increased spatial resolution and retaining a sufficient number of independent depth averages in a bin to estimate an accurate bin average.

d. Surface heat and freshwater fluxes

Mean surface heat fluxes Q from two meteorological reanalysis products are used, the monthly National Centers for Environmental Prediction (NCEP) reanalysis spanning 1948–2000 (Renfrew et al. 2002; Moore and Renfrew 2002) and the Objectively Analyzed Air–Sea Fluxes (OAFlux) spanning 1984–2004 (Yu and Weller 2007). Freshwater flux estimates ($P - E$) are from the NCEP reanalysis. The NCEP reanalysis estimates are calculated on roughly a 2° latitude–longitude grid, and there are five grid points over the MAB shelf (Fig. 1, squares). The OAFlux analysis estimates are on a 1° latitude–longitude grid, and there are 11 grid points over
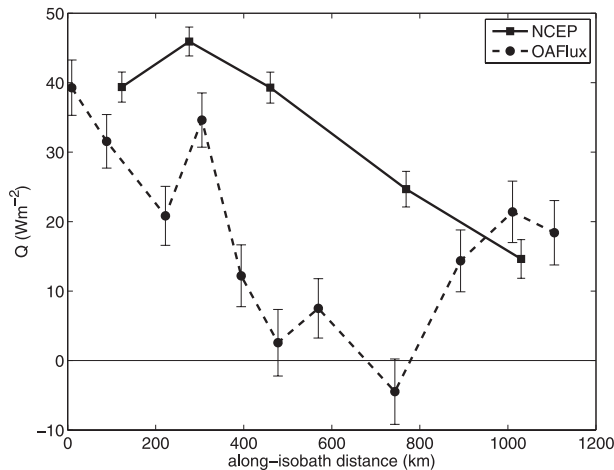
FIG. 2. Mean surface heat fluxes for the MAB from both the NCEP reanalysis (squares) and OAFlux (circles) as a function of distance along the 70-m isobath. Northeast corner of GB is at 0 km and CH is at 1200 km (see Fig. 1 for reanalysis square locations). Error bars indicate 95% CIs based on std error of the means assuming independent monthly values after removal of the annual cycle.
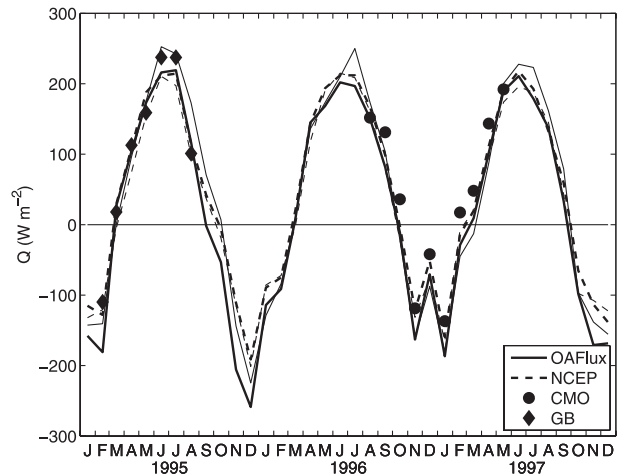

FIG. 3. Monthly averaged surface heat fluxes from NCEP reanalysis (solid line), OAFlux (dashed line), and meteorological buoys deployed on the New England shelf [Coastal Mixing and Optics (CMO) experiment; Lentz et al. 2003b] and southern flank of GB (Lentz et al. 2003a). NCEP and OAFlux surface heat flux estimates for the New England shelf (thick lines) and GB (thin lines) are shown.

the MAB shelf (Fig. 1, circles). A grid point near Cape Hatteras in each reanalysis is not included, because this grid square is primarily in the Gulf Stream and is not representative of the shelf water. Along-isobath surface heat and freshwater flux distributions are determined by interpolating or extrapolating the estimates from the grid points shown in Fig. 1 for each climatology to the center of each along-isobath bin.

Mean surface heat fluxes are, with one exception, positive over the MAB shelf, with values between -5 and 50 W m^{-2}, depending on location and reanalysis product (Fig. 2). The mean surface heat flux is a balance between a relatively large solar heating (165 W m^{-2} from NCEP northern sites) and cooling of a similar magnitude resulting from longwave radiation (-60 W m^{-2}), latent (evaporative) heat loss (-45 W m^{-2}), and sensible heat loss (-20 W m^{-2}). The mean surface heat flux is also small compared to the large annual cycle, with maximum daily averaged net surface heating in June or July in excess of 200 W m^{-2} and net cooling in December or January of about -150 W m^{-2} (Fig. 3). Standard deviations of the year-to-year variations are smaller than the means, $7–11$ W m^{-2}, for the NCEP estimates and similar to the means, $11–18$ W m^{-2}, for the OAFlux estimates. The average surface heat fluxes from NCEP are about 40 W m^{-2} in the north and decrease to approximately 15 W m^{-2} in the south (Fig. 2). The OAFlux estimates decrease more rapidly to a minimum near Hudson Shelf Valley and then increase toward Cape Hatteras. The along-shelf decrease in the net surface heat flux is primarily due to

increases in the mean latent and sensible heat losses from north to south (25 and 10 W m^{-2}, respectively, from NCEP). The north to south increase in the mean latent and sensible heat losses are due to a decrease in the mean air–sea temperature difference, because the mean sea surface temperature increases more rapidly from north to south than the mean air temperature. This heat loss is partially compensated for by an increase in the mean solar radiation from north to south of about 10 W m^{-2}.

The OAFlux average surface heat fluxes are smaller than the NCEP fluxes over most of the MAB shelf. This difference is due in part to the OAFlux estimates having larger latent and sensible heat losses in winter. Mean surface heat flux estimates from Bunker (1976) reported by Beardsley and Boicourt (1981) are similar to the OAFlux estimates and smaller than the NCEP estimates. On a global scale, Yu et al. (2008) report a mean difference between estimates of turbulent surface heat fluxes from 107 buoy time series and the OAFlux estimates of 1 W m^{-2} and a mean difference of 6.3 W m^{-2} between the buoy time series and the NCEP estimates. However, the mean differences between the flux estimates from one buoy time series in the Middle Atlantic Bight and both the OAFlux and NCEP flux estimates were similar: $16–20$ W m^{-2} (see Fig. 16 of Yu et al. 2008). Monthly averages of net surface heat flux from the two climatologies agree reasonably well with estimates from meteorological buoys deployed on the New England shelf (Lentz 2003; note that this is the MAB buoy used in Yu et al. 2008) and southern flank of Georges

Bank (Beardsley et al. 2003; Fig. 3). Mean differences from the buoy estimates are 19 W m^{-2} for the NCEP estimates and 18 W m^{-2} for the OAFlux estimates, which are smaller than the estimated accuracy of the surface flux estimates from the buoys (Beardsley et al. 2003).

The limited existing buoy estimates are not sufficiently long or accurate enough to determine which reanalysis product is more accurate over annual time scales. Therefore, both the NCEP and OAFlux estimates are used in the following analysis. The difference between the two estimates is one measure of the uncertainty of the surface heat flux estimates. Both estimates suffer from coarse spatial resolution relative to the shelf width, so most of the flux squares include both shelf and slope water. Mean surface heat fluxes over the warmer slope water are more negative than those over the cooler shelf waters.

Average precipitation and evaporation rates from the NCEP reanalysis are both about 60 cm yr^{-1} of freshwater over the MAB shelf. As a result, the net freshwater flux ($P - E$) is approximately 1 cm yr^{-1} in the north and -10 cm yr^{-1} in the south, where evaporation is larger. Standard deviations of the year-to-year variations in the freshwater flux are generally larger than the means. Uncertainties in precipitation rates over the ocean are large and almost certainly dominate uncertainty in the surface freshwater flux estimates. For example, comparisons of satellite and NCEP reanalysis estimates of precipitation yield an average relative bias of about 20 cm yr^{-1} over the North Atlantic (Bosilovich et al. 2007). Estimates from ship-based observations yield a mean precipitation rate of 80 cm yr^{-1} (Dorman and Bourke 1981) but a net freshwater flux near zero (Schmitt et al. 1989), similar to the NCEP estimates. Adjacent coastal and island land-based precipitation rates are about 110 cm yr^{-1}, almost twice the NCEP values. However, even if the precipitation rate is doubled to 120 cm yr^{-1} and the same evaporation rate is used, the net freshwater flux is negligible in the along-isobath salt balances discussed in section 4b. This is in part because the net freshwater flux (≈ 100 m^3 s^{-1}) over the MAB shelf (area $\approx 10^{11}$ m^2) is more than an order of magnitude smaller than the average river discharge into the MAB (several thousand cubic meters per second; Beardsley and Boicourt 1981).

4. Results

a. Along-isobath heat balance

Depth-averaged water temperatures (seasonal cycle removed) increase from north to south along the 70-m isobath from an average of 8.5°C over Georges Bank to 12°C offshore of Chesapeake Bay (Fig. 4). Temperature increases more rapidly between Chesapeake Bay and

Cape Hatteras because the 70-m isobath is over the slope where there is warmer slope and Gulf Stream water (e.g., Churchill and Cornillon 1991; Gawarkiewicz et al. 1992; Savidge and Bane 2001; Flagg et al. 2002). Standard deviations of the depth-averaged temperature (100-km along-isobath bins) are relatively constant (1°–1.5°C) from Georges Bank to Delaware Bay and then increase as the 70-m isobath gets near the shelf break and encounters both shelf water and the warmer slope and Gulf Stream water. Occasional, relatively warm, individual depth-averaged temperatures (>15°C) evident throughout the MAB are probably warm salty intrusions of slope water (e.g., Gordon and Aikman 1981; Churchill 1985; Flagg et al. 1994; Lentz et al. 2003c). These general features of the along-isobath distribution of depth-averaged temperatures are also evident along the 30-, 50-, and 90-m isobaths.

To test the hypothesis that the mean surface heat flux is primarily balanced by the mean along-isobath current acting on the mean along-isobath temperature gradient, (2) is integrated along isobath, assuming that $\hat{v}$ is given by (7), to get the along-isobath temperature variation

$$\hat{T}_p(y) = T_o + \int_{y_o}^{y} \frac{Q(y)}{\rho_o C_p h \hat{v}} \, dy, \qquad (8)$$

where $T_o = T(y = y_o)$. Estimates of the along-isobath temperature variation $T_p(y)$ are compared to the observed mean temperature along the 30-, 50-, 70-, and 90-m isobaths using both the NCEP and OAFlux estimates of $Q(y)$ (Fig. 5).

Over the shelf, away from the shelf break, bin-averaged temperatures increase from north to south at a rate of about 4°C (1000 km)$^{-1}$ at the 30-m isobath, decreasing to about 2°C (1000 km)$^{-1}$ at the 70-m isobath (circles in Fig. 5). This is consistent with the model prediction (8) that the along-isobath temperature gradient is inversely proportional to water depth and along-isobath velocity (which increases as the water depth increases). There is an increase in the along-isobath temperature gradient beginning near Cape Hatteras along the 30-m isobath, near Chesapeake Bay along the 50-m isobath, and near Delaware Bay along the 70-m isobath. These increases in the along-isobath temperature gradient all occur where the corresponding depth range (e.g., 60–80 m for the 70-m isobath) reaches the shelf break. The temperature gradient is about 4°C (1000 km)$^{-1}$ along the 90-m isobath, which is near the shelf break throughout the MAB.

Using the NCEP flux estimates in (8), the predicted temperature gradient along the 30-m isobath is similar on average to the observed temperature gradient but too small south of Delaware Bay and too large north of Delaware Bay (thick lines in Fig. 5a). There is close
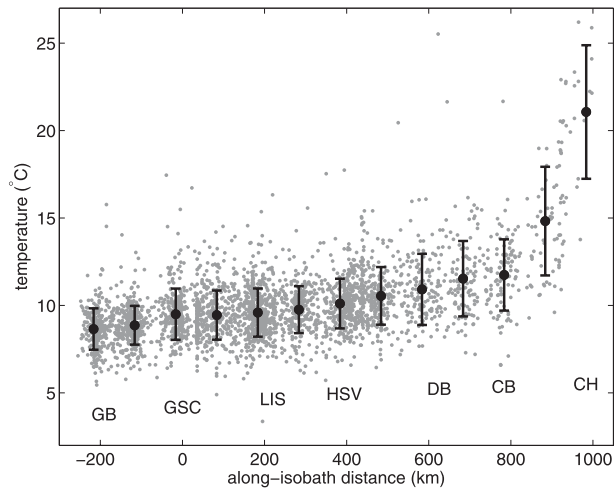
FIG. 4. Individual (small circles) and 100-km along-isobath bin averages (large circles) of depth-averaged temperatures along the 70-m isobath as a function of along-isobath distance relative to Nantucket Shoals. Vertical bars indicate ±1 std dev for each along-isobath bin. The locations of GB, GSC, entrance to LIS, HSV, mouth of DB, mouth of CB, and CH are noted for reference.
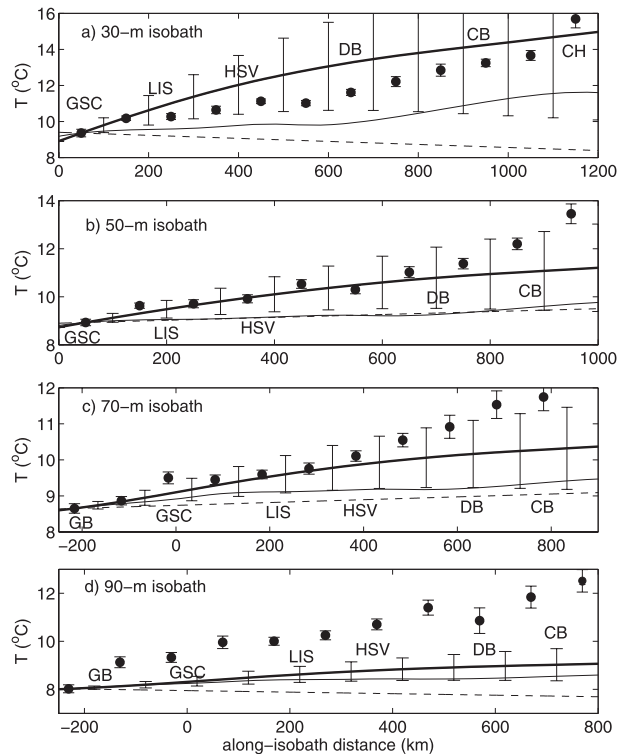

FIG. 5. Bin averages of depth-averaged temperatures (circles) as a function of distance along the (a) 30-, (b) 50-, (c) 70-, and (d) 90-m isobaths. Along-isobath temperature variations resulting from the mean surface heat flux estimated from (8) using NCEP (thick line) and OAFlux (thin line) surface heat fluxes and resulting from the cross-isobath heat flux convergence caused by the mean depth-dependent cross-isobath flow (dashed lines) are also shown. Error bars for depth-averaged temperatures indicate 95% CIs based on std error of the means. Error bars on surface flux estimates (shown for NCEP but also relevant to OAFlux estimates) indicate uncertainty associated with a bias error of ±20 W m^{-2} in surface heat flux. The locations of GB, GSC, entrance to LIS, HSV, mouth of DB, mouth of CB, and CH are noted for reference.

agreement between the predicted and observed temperature gradients along the 50- and 70-m isobaths, except near the shelf break in the south where the temperature rises more rapidly than predicted (Figs. 5b,c). Along the 90-m isobath, which is always near the shelf break, the predicted along-isobath temperature gradient is much smaller than the observed temperature gradient (Fig. 5d).

Using the smaller OAFlux surface heat flux estimates in (8), the predicted temperature gradient underestimates the observed along-isobath temperature increase along all four isobaths (thin lines in Fig. 5). However, the OAFlux estimates reproduce the change in along-isobath temperature gradient along the 30-m isobath (at $y \approx$ 500 km) more closely than the NCEP flux estimates.

Using the NCEP surface flux estimates, the general agreement over the shelf between the predicted along-isobath temperature increase from (8) and the observed along-isobath temperature variation suggests that the mean balance is primarily between surface heating and an along-isobath advective heat flux convergence resulting from the mean depth-averaged flow acting on the mean depth-averaged along-isobath temperature gradient. This implies the other terms in the heat balance, notably the cross-shelf heat flux convergences, are not large. In contrast, the smaller OAFlux surface flux estimates imply a convergent cross-shelf heat flux is required to balance the along-isobath heat flux divergence. The sensitivity of these results to the relatively small differences in the net surface heat flux estimates from the NCEP and OAFlux reanalyses highlights the need for

more accurate surface heat flux estimates over the continental shelf to determine the mean heat balance and the associated structure of the mean temperature field. The discrepancy between the observed and predicted along-isobath temperature gradient near the shelf break using either surface heat flux estimate is not surprising because the observed temperature gradient is probably due to inclusion of more slope water in the bin averages toward the south, an increase in the slope water temperatures to the south, and the closer proximity to the warmer Gulf Stream toward the south.

b. Along-isobath salt balance

Similar to the depth-averaged temperatures, depth-averaged salinities along the 70-m isobath increase steadily from about 32.5 over Georges Bank to 33.5 offshore of
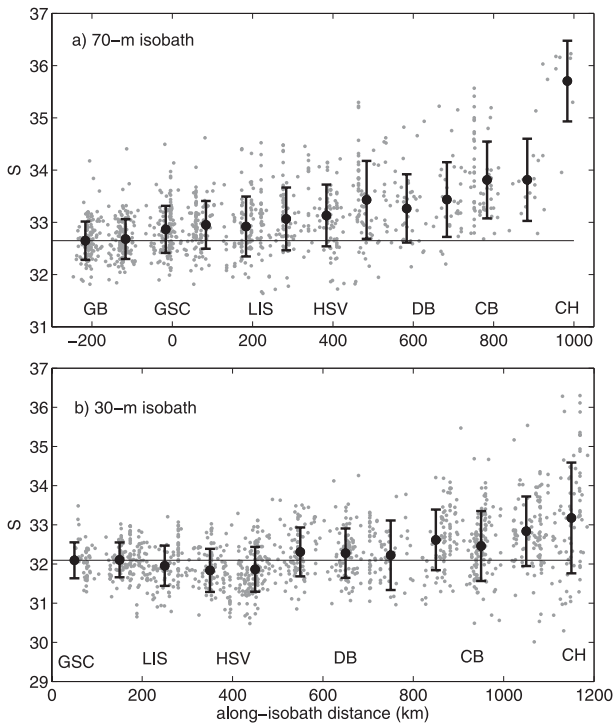
FIG. 6. Individual (small circles) and along-isobath bin averages (large circles) of depth-averaged salinities along the (a) 70- and (b) 30-m isobaths as a function of along-isobath distance relative to Nantucket Shoals. Vertical bars indicate ±1 std dev for each along-isobath bin. The locations of GB, GSC, entrance to LIS, HSV, mouth of DB, mouth of CB, and CH are noted for reference.
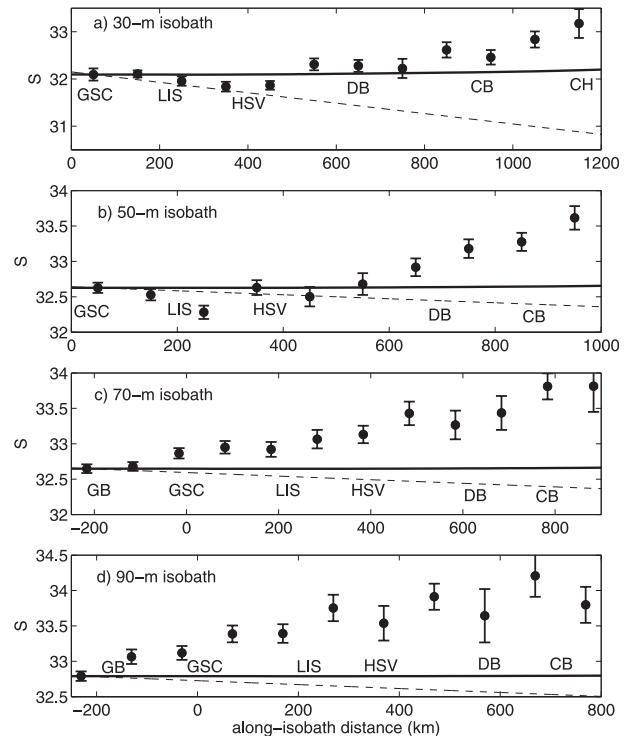

FIG. 7. Bin averages of depth-averaged salinities (circles) and channel model estimate of salinity change resulting from evaporation and precipitation from (9) (line) as a function of distance along the (a) 30-, (b) 50-, (c) 70-, and (d) 90-m isobaths. Estimates of the salinity change caused by the cross-isobath salt flux convergence resulting from the mean depth-dependent cross-isobath flow are also shown (dashed lines). Error bars for the bin-averaged salinities indicate 95% CIs based on std error of the means. Error bars are not shown for surface freshwater flux estimates because the surface flux is negligible even for an uncertainty of ±100%. The locations of GB, GSC, entrance to LIS, HSV, mouth of DB, mouth of CB, and CH are noted for reference.

Chesapeake Bay and then rise rapidly near Cape Hatteras because of the proximity of the Gulf Stream (Fig. 6a). There are relatively few individual depth-averaged salinities in the southern portion of the MAB because the 70-m isobath is over the slope and consequently the isobath band (60–80 m) is narrow. Standard deviations increase from 0.5 in the north to 0.8 in the south. There are a few intermittent high salinity values (>34) presumably associated with warm salty intrusions of slope water as noted for temperature.

Depth-averaged salinities along the 30-m isobath decrease from Great South Channel to Hudson Shelf Valley and then increase on average from Hudson Shelf Valley to Cape Hatteras (Fig. 6b). However, low-salinity values (<31) are evident near the entrance to Long Island Sound, near the mouth of the Hudson River (at the head of Hudson Shelf Valley), and south of Chesapeake Bay because of freshwater discharge and the tendency for the 30-m isobath band to be close to shore in these areas and hence include the associated buoyant coastal currents (e.g., Rennie et al. 1999; Codiga 2005; Chant et al. 2008; Castelao et al. 2008). The lack of low salinities south of Delaware Bay is probably due to the 30-m isobath

band remaining offshore of the buoyant coastal current (Munchow and Garvine 1993).

Mean depth-averaged salinities tend to increase along isobath from north to south at a rate of 1–1.5 $(1000 \text{ km})^{-1}$ throughout the MAB along the 70- and 90-m isobaths and south of Hudson Shelf Valley along the 30- and 50-m isobaths (circles in Fig. 7). Mean salinities decrease along the 30-m isobath from Nantucket Shoals to Hudson Shelf Valley and are relatively fresh near the entrance to Long Island Sound and near Hudson Shelf Valley along the 50-m isobath. Changes in the along-isobath salinity gradient associated with proximity to the shelf-slope front are not as obvious as they are for depth-averaged temperatures.

Estimates of the along-isobath salinity variation based on along-isobath integration of (3),

$$\hat{S}_p(y) = S(y = y_o) - \int_{y_o}^{y} \frac{[P(y) - E(y)]S_o}{h\hat{v}} \, dy, \quad (9)$$
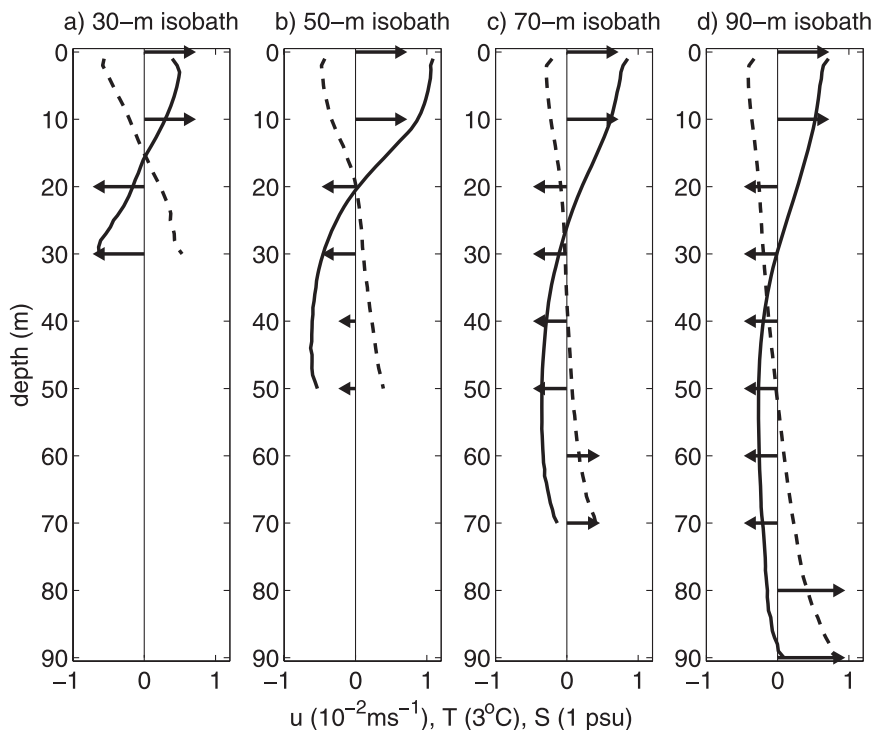
FIG. 8. Examples of the mean temperature (*T*; solid lines), salinity (*S*; dashed lines), and cross-shelf current (*u*; arrows) profiles at the (a) 30-, (b) 50-, (c) 70-, and (d) 90-m isobaths used to estimate the cross-shelf heat and salt fluxes shown in Fig. 9. The temperature profiles are relative to mean depth-averaged temperatures of 12.0°C at the 30-m isobath, 10.3°C at the 50-m isobath, 9.5°C at the 70-m isobath, and 9.5°C at the 90-m isobath, with corresponding temperature ranges of 3.5°, 5.1°, 3.6°, and 2.9°C. The salinity profiles are relative to mean depth-averaged salinities of 32.3 at the 30-m isobath, 32.7 at the 50-m isobath, 32.8 at the 70-m isobath, and 33.1 at the 90-m isobath, with corresponding salinity ranges of 1.1, 0.9, 0.7, and 1.2. Cross-shelf velocity profiles are from a simple model described in the appendix.

and the freshwater flux from the NCEP reanalysis predict essentially no along-isobath variation in depth-averaged salinity because $P - E$ is small (thick lines in Fig. 7). The along-isobath increase in salinity over much of the MAB shelf is almost certainly due to an onshore flux of salt, because the surface flux $(P - E)$ is small, the coastal river discharge decreases the salinity, and it seems unlikely that there would be a significant northward along-isobath "eddy" salt flux against the southward along-isobath mean flow. Previous studies have argued for an onshore flux of salt to compensate for the freshwater runoff into the MAB (Wright 1976). The along-isobath salinity increase to the south suggests the onshore flux of salt must be larger than what would be needed to compensate for the river discharge into the MAB.

5. Discussion

a. Cross-isobath heat flux

Climatological analyses indicate there are substantial mean cross-isobath temperature and salinity gradients,

as well as along-isobath gradients (e.g., see Linder et al. 2006 for pictures of the seasonal mean temperature and salinity fields at middepth in the MAB). The component of the cross-isobath heat flux resulting from the mean cross-shelf velocity profile acting on the mean temperature profile is estimated to determine whether it can account for the cross-isobath heat flux convergence implied by the OAFlux surface heat flux estimates or is small as suggested by the NCEP surface heat flux estimates. A rough estimate of the cross-isobath heat flux resulting from the product of the mean, depth-dependent, cross-shelf velocity and temperature profiles,

$$H^x = \int_{-h}^{0} \tilde{u}\tilde{T}\, dz,$$

can be made using the observed mean temperature profiles (Fig. 8, solid lines) and a simple model of the mean cross-shelf velocity profile (Fig. 8, arrows; Lentz 2008). Lentz (2008) showed that observed mean cross-shelf velocity profiles are consistent with a three-component
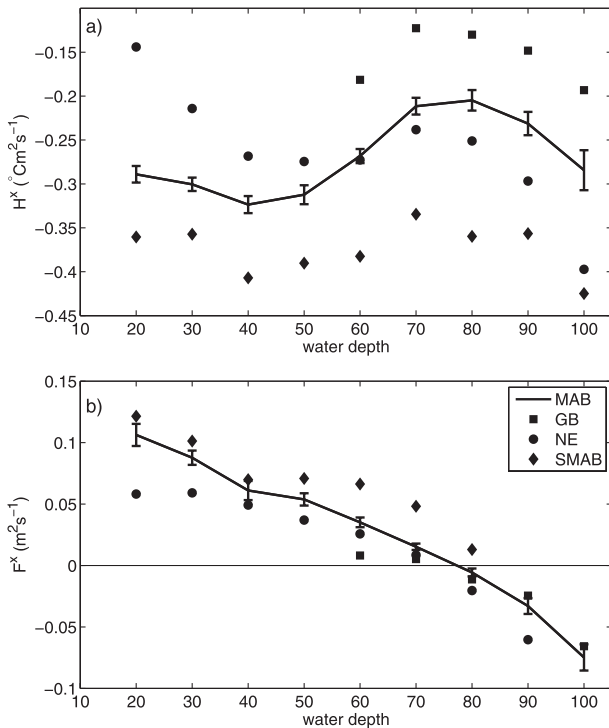
FIG. 9. Estimates of the average cross-isobath (a) heat flux $H^x = \int \tilde{u}\tilde{T}\,dz$ [Eq. (A3)] and (b) salt flux $F^x = \int \tilde{u}\tilde{S}\,dz$ [Eq. (A4)] as functions of water depth. Symbols indicate estimates for GB (east of 69.5°W), the New England shelf (between HSV and GSC), and the southern MAB (south of HSV). Error bars indicate 95% CIs based on std error of the means.

flow: 1) a vertically uniform geostrophic onshore flow associated with a mean along-isobath pressure gradient; 2) a mean offshore flow in the surface boundary layer given by the Ekman transport resulting from the wind stress; and 3) a mean offshore flow in the bottom boundary layer given by the Ekman transport resulting from the bottom stress. The inferred mean along-isobath pressure gradient must be due to an along-isobath sea surface slope because hydrographic data indicate that there is not a measureable mean depth-averaged along-isobath density gradient (see section 5c and Fig. 10). The offshore transport in the bottom boundary layer increases with distance offshore. Consequently, the near-bottom flow, which is the sum of the interior onshore flow and the offshore flow in the bottom Ekman layer, is onshore between the coast and the 50-m isobath and offshore seaward of the 50-m isobath (Bumpus 1965; Lentz 2008). Estimation of the resulting cross-isobath heat and salt flux is described in the appendix.

There is a relatively constant offshore flux of heat (H^x is −0.2 to −0.3°C m² s⁻¹) between the 20- and 100-m isobaths (Fig. 9a) because of the offshore flow of warmer near-surface water and the onshore flow of colder water

below the surface boundary layer (Fig. 8). There is a minimum at the 40- or 50-m isobath, where the temperature and velocity anomaly profiles (relative to depth averages) have a similar vertical structure (Fig. 8b), and there is a maximum at the 70- or 80-m isobath, where the temperature anomaly profile has a two-layer structure and the cross-shelf velocity profile has a three-layer structure (Fig. 8c). The magnitude of H^x increases from Georges Bank (Fig. 9a, squares) to the southern MAB (triangles); however, the pattern and cross-isobath gradients are similar in each region. The negative values of $H^x \approx -0.3$°C m² s⁻¹ at the 20-m isobath imply a relatively large export of heat from the inner shelf because $H^x = 0$ at the coast. This is qualitatively consistent with results of a recent study indicating that there is a mean offshore heat flux resulting from the cross-shelf circulation that balances surface heating over the inner shelf south of Martha's Vineyard during summer (Fewings and Lentz 2009, manuscript submitted to *J. Geophys. Res.*).

The cross-isobath heat flux gradient $\partial H^x/\partial x$ was estimated from the cross-isobath dependence on water depth by assuming a constant bottom slope ($\partial h/\partial x = -6 \times 10^{-4}$). To estimate the contribution of $\partial H^x/\partial x$ to the along-isobath change in temperature, $\partial H^x/\partial x$ is assumed to be uniform along isobath and integrated as in (8), with $Q/\rho_o C_p$ replaced by $-\partial H^x/\partial x$. The negative cross-isobath heat flux gradients over the inner and outer shelf imply cooling and hence a slight temperature decrease from north to south (Figs. 5a,d, dashed lines), whereas the positive gradient at midshelf suggests a slight temperature increase (Figs. 5b,c, dashed lines).

Along all four isobaths, the along-isobath temperature variations resulting from $\partial H^x/\partial x$ are small compared to the observed along-isobath temperature gradient (Fig. 5, compare the dashed lines to the circles). The small $\partial H^x/\partial x$ resulting from the mean cross-shelf circulation is consistent with the assumed balance between surface heating estimated from NCEP and along-isobath advection over the midshelf and outer shelf. If the OAFlux estimates of surface heating are more accurate, the small $\partial H^x/\partial x$ does not account for the discrepancy between the surface heating and along-isobath advection, which suggests that eddy heat fluxes are important. The onshore eddy heat (temperature) flux at the 100-m isobath (shelf break) required to close the heat balance in this case (using OAFlux estimates) is 0.5°–0.9°C m² s⁻¹, assuming a constant cross-shelf heat flux gradient and no flux at the coast. The corresponding eddy heat flux per unit width and depth is 0.2×10^{-5} to 0.4×10^{-5} W m⁻², which is similar to a bulk estimate reported by Houghton et al. (1988; 0.32×10^{-5} W m⁻²) and estimates from hydrographic surveys at the shelfbreak front reported by Garvine et al. (1989) and Gawarkiewicz et al. (2004;

0.23×10^{-5} and 0.16×10^{-5} W m^{-2}, respectively), though both these estimates are not significantly different from zero.

b. Cross-isobath salt flux

Estimates of the corresponding cross-isobath salt flux,

$$F^x = \int_{-h}^{0} \tilde{u}\tilde{S} \, dz,$$

resulting from the mean cross-shelf circulation (Fig. 8, arrows) acting on the mean salinity profiles (Fig. 8, dashed lines) indicate an onshore flux of salt ($F^x > 0$) at the 20-m isobath decreasing monotonically across the shelf to an offshore flux of salt ($F^x < 0$) over the outer shelf (Fig. 9b). The positive salt flux at the 20-m isobath (Fig. 9b) implies an onshore flux of salt into the inner shelf caused by the offshore flow of fresher near-surface water and the onshore flow of saltier near-bottom water (Fig. 8a). This onshore salt flux may balance the freshwater flux onto the MAB shelf from rivers and estuaries. The salt flux is approximately zero near the 70-m isobath because the offshore flux of relatively fresh near-surface water is balanced by an offshore flux of relatively salty near-bottom water (Fig. 8c). Farther offshore, the salt flux is offshore (negative) because the offshore flux of relatively salty near-bottom water exceeds the offshore flux of relatively fresh near-surface water (Fig. 8d).

The cross-isobath salt flux gradient, $\partial F^x/\partial x \approx -10^{-6}$ m s^{-1}, is positive (x positive onshore), relatively constant, and similar in the different regions of the MAB. Assuming $\partial F^x/\partial x$ is uniform along isobath and replacing the surface flux in (9) with $-\partial F^x/\partial x$, the salt flux divergence implies an along-isobath decrease in salinity from north to south (Fig. 7, dashed lines). The implied along-isobath salinity decrease is similar in magnitude to the along-isobath salinity variation along the 30-m isobath and is relatively small along the 50-, 70-, and 90-m isobaths. This implies there must be an eddy salt flux convergence to account for both the along-isobath salinity increase and the salt flux divergence resulting from the mean cross-shelf circulation. The onshore eddy salt flux at the 100-m isobath (shelfbreak) required to close the salt balance along the 50- and 70-m isobaths is about 0.7 m^2 s^{-1}, assuming a constant cross-shelf salt flux gradient and no flux at the coast. The corresponding eddy salt flux per unit width and depth is 0.7×10^{-2} kg m^{-2} s^{-2}, the same as the onshore eddy salt flux estimate from repeated hydrographic surveys reported by Gawarkiewicz et al. (2004). The close agreement is probably fortuitous, given the uncertainties in both estimates. Houghton et al. (1988) reported a value of 0.22×10^{-2} kg m^{-2} s^{-2},
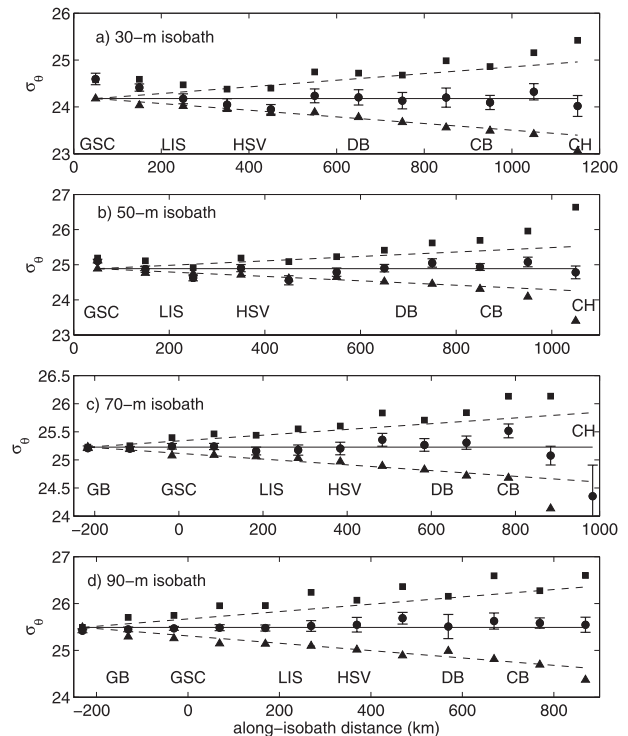

FIG. 10. Bin averages of depth-averaged densities (circles) are shown; also shown are the temperature (αT; $\alpha = -0.18$ kg m^{-3} °C^{-1}; triangles) and salinity (βS; $\beta = 0.78$ kg m^{-3}; squares) contributions to density as a function of distance along the (a) 30-, (b) 50-, (c) 70-, and (d) 90-m isobaths. Dashed lines are linear fits to αT over the range where bin averages appear linear. Error bars for density indicate 95% CIs based on std error of the means. The locations of GB, GSC, entrance to LIS, HSV, mouth of DB, mouth of CB, and CH are noted for reference.

whereas Garvine et al. (1989) found a small offshore salt flux that was not significantly different from zero.

c. Along-isobath density gradient and implications of TS compensation

In contrast to temperature and salinity, there is generally not a significant along-isobath density gradient over the MAB shelf, because the density decrease resulting from the along-isobath temperature gradient balances the density increase because of the along-isobath salinity gradient (Fig. 10). This tendency for the density contributions from the along-isobath temperature and salinity gradients to compensate is intriguing. Compensating horizontal temperature and salinity gradients have been observed in the surface mixed layer of the open ocean (e.g., Rudnick and Ferrari 1999). The tendency for compensation has been attributed to horizontal shear dispersion associated with slumping of horizontal density gradients leaving behind temperature and salinity gradients that have no associated density signature (Young

1994). Whether some form of this process accounts for the observed along-isobath compensation in the MAB over scales of 1000 km is unclear (see footnote 15 in Rudnick and Ferrari 1999).

It is worth emphasizing that a given volume exchange will not generally result in density compensating exchanges of heat and salt, because the cross-shelf temperature and salinity gradients do not compensate for each other (i.e., there is a cross-shelf density gradient). This is clearly evident from the results in sections 5a and 5b, where the same mean cross-shelf circulation (Fig. 8) results in heat and salt fluxes (Fig. 9) with very different buoyancy (density) flux magnitudes and cross-shelf structures. The heat flux is negative across the entire shelf, whereas the salt flux changes sign.

The results in section 4a suggest the along-isobath temperature gradient is partially (OAFlux estimates) or primarily (NCEP estimates) determined by the surface heat flux and the along-isobath flow. This, in turn, suggests a feedback mechanism that generates a salt flux convergence that results in an along-isobath salinity gradient large enough to compensate for the along-isobath temperature gradient. One possible feedback mechanism is that the salt and heat fluxes driven by the cross-isobath circulation in thermal wind balance with a given along-isobath density gradient could erase that along-isobath density gradient.

The cross-isobath flow in thermal wind balance with a vertically uniform along-isobath density gradient, assuming no net cross-isobath volume transport, is

$$u_g = \frac{g\rho_y}{f\rho_o}\left(z + \frac{h}{2}\right),\tag{10}$$

where g is acceleration due to gravity and f is the Coriolis frequency, starting with a negative along-isobath density gradient (i.e., $\rho_y < 0$) due only to the observed along-isobath temperature gradient (Fig. 10, triangles) and with no initial along-isobath salinity gradient. This negative density gradient implies from (10) an offshore thermal wind flow in the upper half of the water column and an onshore flow in the lower half of the water column. This cross-isobath circulation drives an offshore transport of less salty near-surface water that is replaced by an onshore transport of saltier near-bottom water resulting in an onshore flux of salt. The salt flux convergence would result in an along-isobath salinity gradient that would tend to compensate for the along-isobath temperature gradient. As the density gradient decreased, the cross-shelf circulation would decrease; therefore, the onshore salt flux would decrease. There would also be an offshore flux of heat that would tend to reduce the density gradient if water temperature decreases with depth.

Although clearly overidealized, this simple model suggests one potential feedback mechanism that would push the system toward no along-isobath density gradient. Determining the implications of this feedback mechanism to the equilibrium structure of the temperature, salinity, and flow fields is beyond the scope of this study but would be interesting to pursue using a numerical model with more complete physics.

6. Summary

The mean heat and salt balances for the Middle Atlantic Bight continental shelf are studied using historical temperature and salinity profiles from ships and surface heat and freshwater fluxes from the NCEP (heat and freshwater flux) and OAFlux (heat flux) reanalyses of historical meteorological data. Specifically, the hypothesis is tested that the mean surface heat and freshwater fluxes are balanced by along-isobath fluxes resulting from the mean equatorward along-shelf flow in the MAB. In a Lagrangian frame, this is equivalent in the case of the heat balance to a column of water warming due to surface heating as it flows from north to south along the MAB continental shelf.

The mean depth-averaged temperature increases along isobath from north to south at a rate of $4°C\ (1000\ \mathrm{km})^{-1}$ along the 30-m isobath, decreasing to $2°C\ (1000\ \mathrm{km})^{-1}$ along the 70-m isobath (Fig. 5, circles; the along-isobath extent of the MAB is roughly 1000 km). The hypothesized mean heat balance,

$$\hat{v}h\hat{T}_y = \frac{Q}{\rho_o C_p},$$

reproduces the observed along-isobath temperature gradient over the MAB shelf along the 50- and 70-m isobaths using the mean surface heat flux Q from the NCEP reanalysis, whereas the smaller OAFlux estimates of Q underestimate the along-isobath temperature gradient (Fig. 5, solid lines). Thus, the NCEP surface heat flux estimates imply that the mean cross-shelf heat flux divergence is small compared to the surface heat flux, whereas the OAFlux estimates imply a mean cross-shelf heat flux convergence that warms the shelf at a rate similar to the surface heat flux. It is unclear whether the NCEP or OAFlux surface heat flux estimates are more accurate, but the importance of the small differences ($10–20\ \mathrm{W\ m}^{-2}$) between them to the mean heat balance emphasizes the need for more accurate surface heat flux estimates for the MAB continental shelf. Estimates of the component of the cross-shelf heat flux divergence resulting from the mean cross-shelf circulation are small relative to the along-isobath heat flux divergence (Fig. 5, dashed lines).

Mean depth-averaged salinities increase along isobath from north to south at a rate of about 1.5 $(1000 \text{ km})^{-1}$ throughout the MAB along the 70- and 90-m isobaths and south of Hudson Shelf Valley along the 30- and 50-m isobaths (Fig. 7, circles). Surface freshwater fluxes (precipitation minus evaporation) from the NCEP reanalysis are too small to account for the observed along-isobath salinity gradients (Fig. 7, lines). Estimates of the cross-shelf salt flux divergence resulting from the mean cross-shelf circulation are substantial but are the wrong sign to account for the observed along-isobath salinity increase (Fig. 7, dashed lines). These results combined with the river discharge onto the MAB shelf imply that there must be an onshore eddy salt flux throughout the MAB.

The along-isobath temperature and salinity gradients tend to compensate so that the mean along-isobath depth-averaged density gradient is approximately zero (Fig. 10). This tendency for temperature and salinity gradients to compensate suggests there may be a feedback mechanism such that any along-isobath density gradient generates advective onshore salt and heat fluxes that, in turn, tend to reduce or eliminate the along-isobath density gradient.

The lack of current observations suitable for studies focusing on time scales of years or longer (e.g., Lentz 2008) severely limits our ability to make progress in understanding the heat and salt balances and the associated temperature and salinity distributions because of our inability to directly estimate mean advective heat and salt fluxes. The hope is that this study provides motivation and a basis for subsequent numerical modeling studies of the MAB heat and salt balances (e.g., Wilkin 2006).

APPENDIX

Estimation of Cross-Isobath Heat Flux

The mean cross-isobath heat and salt flux divergences resulting from the mean cross-isobath current profile acting on the mean temperature or salinity profiles (Fig. 8) are estimated using the historical hydrographic profiles and a model of the mean cross-isobath current structure (Lentz 2008). Following Lentz (2008), the mean cross-isobath volume transport is represented by surface and bottom Ekman transports ($U^s = \tau^{sy}/\rho_o f$ and $U^b = -\tau^{by}/\rho_o f$) and a geostrophic interior transport $U^i = -gh\eta_y/f$, and the net cross-isobath transport is assumed to be zero (Dever 1997; Lentz 2008):

$$U^s + U^i + U^b = u^s\delta^s + u^i h + u^b\delta^b = 0. \quad (A1)$$

Here, τ^{sy} and τ^{by} are the along-isobath wind and bottom stress, f is the Coriolis frequency, g is gravitational acceleration, η_y is the along-isobath sea surface slope, u^s and u^b are the Ekman velocities in the surface and bottom boundary layers, u^i is the interior geostrophic velocity, and δ^s and δ^b are surface and bottom boundary layer thicknesses. The cross-isobath heat flux resulting from the mean cross-shelf circulation is

$$H^x = \int_{-h}^{0} \tilde{u}\tilde{T}\,dz = \int_{-\delta^s}^{0} u^s\tilde{T}\,dz$$
$$+ \int_{-h}^{0} u^i\tilde{T}\,dz + \int_{-h}^{\delta^b-h} u^b\tilde{T}\,dz. \quad (A2)$$

Assume the boundary layers are mixed layers, so temperature is vertically uniform in the surface and bottom boundary layers, and the alongshore pressure gradient $g\eta_y$ is vertically uniform (see section 5c), so the geostrophic interior velocity $u^i = -g\eta_y/f$ is also vertically uniform. Then (A2) reduces to

$$H^x = \int_{-h}^{0} \tilde{u}\tilde{T}\,dz = U^s T^s + U^i\hat{T} + U^b T^b$$
$$= U^s(T^s - T^b) + U^i(\hat{T} - T^b), \quad (A3)$$

where T^s and T^b are the temperatures in the surface and bottom mixed layers, $\hat{T}$ is the depth-averaged temperature, and (A1) is used to replace U^b. The corresponding cross-isobath salt flux is

$$F^x = \int_{-h}^{0} \tilde{u}\tilde{S}\,dz = U^s(S^s - S^b) + U^i(\hat{S} - S^b). \quad (A4)$$

Cross-isobath heat and salt fluxes are estimated from (A3) and (A4) for 10-m isobath intervals from the 20-m isobath to the 100-m isobath. Following Lentz (2008), a mean wind stress of $\tau^{sy} = -0.015$ N m^{-2} is used to estimate U^s and a mean sea surface slope of $\eta_y = -3.7 \times 10^{-8}$ is used to estimate U^i. The mean $\hat{T}$, T^s, and T^b (or $\hat{S}$, S^s, and S^b) are calculated for all profiles within ± 5 m of a given isobath. The transport and mean temperature or salinity values provide estimates of the average H^x or F^x along a given isobath within the MAB. To determine whether there are along-isobath variations in H^x and F^x, the estimates were also calculated for three subregions, Georges Bank, the New England shelf (between Hudson Shelf Valley and Great South Channel), and the southern MAB (between Hudson Shelf Valley and Cape Hatteras).

REFERENCES

Austin, J. A., and S. J. Lentz, 1999: The relationship between synoptic weather systems and meteorological forcing on the North Carolina inner shelf. *J. Geophys. Res.,* **104,** 18 159–18 186.

Beardsley, R. C., and W. C. Boicourt, 1981: On estuarine and continental-shelf circulation in the Middle Atlantic Bight. *Evolution of Physical Oceanography, Scientific Surveys in Honor of Henry Stommel,* B. A. Warren and C. Wunsch, Eds., MIT Press, 198–233.

——, ——, and D. V. Hansen, 1976: Physical oceanography of the Middle Atlantic Bight. *Proceedings of the Symposium on Middle Atlantic Continental Shelf and the New York Bight,* Vol. 2, M. G. Gross, Ed., American Society of Limnology and Oceanography, 20–34.

——, D. C. Chapman, K. H. Brink, S. R. Ramp, and R. Schlitz, 1985: The Nantucket Shoals Flux Experiment (NSFE79). Part I: A basic description of the current and temperature variability. *J. Phys. Oceanogr.,* **15,** 713–748.

——, S. J. Lentz, R. A. Weller, R. Limeburner, J. D. Irish, and J. B. Edson, 2003: Surface forcing on the southern flank of Georges Bank, February–August 1995. *J. Geophys. Res.,* **108,** 8007, doi:10.1029/2002JC001359.

Bigelow, H. B., 1933: Studies of the waters on the continental shelf, Cape Cod to Chesapeake Bay. I. The cycle of temperature. *Pap. Phys. Oceanogr. Meteor.,* **2,** 1–135.

——, and M. Sears, 1935: Studies of the waters on the continental shelf, Cape Cod to Chesapeake Bay. II. Salinity. *Pap. Phys. Oceanogr. Meteor.,* **4,** 1–94.

Bignami, F., and T. S. Hopkins, 2003: Salt and heat trends in the shelf waters of the southern Middle-Atlantic Bight. *Cont. Shelf Res.,* **23,** 647–667.

Bosilovich, M. G., J. Chen, F. R. Robertson, and R. F. Adler, 2007: Evaluation of global precipitation in reanalyses. Preprints, *21st Conf. on Hydrology,* San Antonio, TX, Amer. Meteor. Soc., 1.6. [Available online at http://ams.confex.com/ams/pdfpapers/118494.pdf.]

Brink, K. H., 1998: Deep-sea forcing and exchange processes. *The Sea—Ideas and Observations on Progress in the Study of the Seas,* K. H. Brink and A. R. Robinson, Eds., Vol. 10, *The Global Coastal Ocean,* John Wiley and Sons, 151–167.

Bumpus, D. F., 1965: Residual drift along the bottom on the continental shelf in the Middle Atlantic Bight area. *Limnol. Oceanogr.,* **10,** R50–R53.

——, 1973: A description of the circulation on the continental shelf of the east coast of the United States. *Progress in Oceanography,* B. A. Warren, Ed., Pergamon Press, 111–157.

Bunker, A. F., 1976: Computations of surface energy flux and annual air-sea interaction cycles of the North Atlantic Ocean. *Mon. Wea. Rev.,* **104,** 1122–1140.

Butman, B., and R. C. Beardsley, 1987: Long-term observations on the southern flank of Georges Bank. Part I: A description of the seasonal cycle of currents, temperature, stratification, and wind stress. *J. Phys. Oceanogr.,* **17,** 367–384.

Castelao, R., O. Schofield, S. Glenn, R. Chant, and J. Kohut, 2008: Cross-shelf transport of freshwater on the New Jersey shelf. *J. Geophys. Res.,* **113,** C07017, doi:10.1029/2007JC004241.

Chant, R. J., S. M. Glenn, E. Hunter, J. Kohut, R. F. Chen, R. W. Houghton, J. Bosch, and O. Schofield, 2008: Bulge formation of a buoyant river outflow. *J. Geophys. Res.,* **113,** C01017, doi:10.1029/2007JC004100.

Churchill, J. H., 1985: Intrusions of outer shelf and slope water with the nearshore zone off Long Island, New York. *Limnol. Oceanogr.,* **30,** 972–986.

——, and P. C. Cornillon, 1991: Gulf Stream water on the shelf and upper slope north of Cape Hatteras. *Cont. Shelf Res.,* **11,** 409–431.

Codiga, D. L., 2005: Interplay of wind forcing and buoyant discharge off Montauk Point: Seasonal changes to velocity structure and a coastal front. *J. Phys. Oceanogr.,* **35,** 1068–1085.

Csanady, G. T., and B. A. Magnell, 1987: Mixing processes. *Georges Bank,* R. H. Backus, Ed., MIT Press, 163–169.

Dever, E. P., 1997: Wind-forced cross-shelf circulation on the northern California shelf. *J. Phys. Oceanogr.,* **27,** 1566–1580.

Dorman, C. E., and R. H. Bourke, 1981: Precipitation over the Atlantic Ocean, 30°S to 70°N. *Mon. Wea. Rev.,* **109,** 554–563.

Fewings, M., S. J. Lentz, and J. Fredericks, 2008: Observations of cross-shelf flow driven by cross-shelf winds on the inner continental shelf. *J. Phys. Oceanogr.,* **38,** 2358–2378.

Flagg, C. N., R. W. Houghton, and L. J. Pietrafesa, 1994: Summertime thermocline salinity maximum intrusions in the Mid-Atlantic Bight. *Deep-Sea Res.,* **41,** 325–340.

——, L. J. Pietrafesa, and G. L. Weatherly, 2002: Springtime hydrography of the southern Middle Atlantic Bight and the onset of seasonal stratification. *Deep-Sea Res.,* **49,** 4297–4329.

Garvine, R. W., K.-C. Wong, and G. G. Gawarkiewicz, 1989: Quantitative properties of shelfbreak eddies. *J. Geophys. Res.,* **94,** 14 475–14 483.

Gawarkiewicz, G., T. M. Church, G. W. Luther III, T. G. Ferdelman, and M. Caruso, 1992: Large-scale penetration of Gulf Stream water onto the continental shelf north of Cape Hatteras. *Geophys. Res. Lett.,* **19,** 373–376.

——, K. H. Brink, F. Bahr, R. C. Beardsley, M. Caruso, J. F. Lynch, and C.-S. Chiu, 2004: A large-amplitude meander of the shelfbreak front during summer south of New England: Observations from the Shelfbreak PRIMER experiment. *J. Geophys. Res.,* **109,** C03006, doi:10.1029/2002JC001468.

Gordon, A. L., and F. Aikman III, 1981: Salinity maximum in the pycnocline of the Middle Atlantic Bight. *Limnol. Oceanogr.,* **26,** 123–130.

Houghton, R. W., F. Aikman III, and H. W. Ou, 1988: Shelf-slope frontal structure and cross-shelf exchange at the New England shelf-break. *Cont. Shelf Res.,* **8,** 687–710.

Joyce, T. M., 1987: Meteorology and air-sea interactions. *The Marine Environment of the U.S. Atlantic Continental Slope and Rise,* J. D. Milliman and W. R. Wright, Eds., Jones and Bartlett, 5–26.

——, C. Deser, and M. A. Spall, 2000: The relation between decadal variability of subtropical mode water and the North Atlantic Oscillation. *J. Climate,* **13,** 2550–2569.

Lentz, S. J., 2003: A climatology of salty intrusions over the continental shelf from Georges Bank to Cape Hatteras. *J. Geophys. Res.,* **108,** 3326, doi:10.1029/2003JC001859.

——, 2008: Observations of the mean circulation over the Middle Atlantic Bight continental shelf. *J. Phys. Oceanogr.,* **38,** 1203–1221.

——, R. C. Beardsley, J. D. Irish, J. Manning, P. C. Smith, and R. A. Weller, 2003a: Temperature and salt balances on Georges Bank February–August 1995. *J. Geophys. Res.,* **108,** 8006, doi:10.1029/2001JC001220.

——, S. Elgar, and R. T. Guza, 2003b: Observations of the flow field near the nose of a buoyant coastal current. *J. Phys. Oceanogr.,* **33,** 933–943.

——, K. Shearman, S. Anderson, A. Plueddemann, and J. Edson, 2003c: The evolution of stratification over the New England shelf during the Coastal Mixing and Optics study, August 1996–June 1997. *J. Geophys. Res.,* **108,** 3008, doi:10.1029/2001JC001121.

Linder, C. A., and G. Gawarkiewicz, 1998: A climatology of the shelfbreak front in the Middle Atlantic Bight. *J. Geophys. Res.,* **103,** 18 405–18 423.

——, ——, and M. Taylor, 2006: Climatological estimation of environmental uncertainty over the Middle Atlantic Bight shelf and slope. *IEEE J. Oceanic Eng.,* **31,** 308–324.

Loder, J. W., B. Petrie, and G. Gawarkiewicz, 1998: The coastal ocean off northeastern North America: A large-scale view. *The Sea: The Global Coastal Ocean,* A. R. Robinson and K. H. Brink, Eds., Regional Studies and Syntheses, Vol. 11, Wiley, 105–133.

Manning, J., 1991: Middle Atlantic Bight salinity: Interannual variability. *Cont. Shelf Res.,* **11,** 123–137.

Maul, G., A. Davis, and J. Simmons, 2001: Seawater temperature trends at USA tide gauge sites. *Geophys. Res. Lett.,* **28,** 3935–3937.

Mayer, D. A., D. V. Hansen, and D. A. Ortman, 1979: Long-term current and temperature observation on the Middle Atlantic shelf. *J. Geophys. Res.,* **84,** 1776–1792.

Moore, G. W. K., and I. A. Renfrew, 2002: An assessment of the surface turbulent heat fluxes from the NCEP–NCAR reanalysis over the western boundary currents. *J. Climate,* **15,** 2020–2037.

Mountain, D. G., 2003: Variability in the properties of Shelf Water in the Middle Atlantic Bight, 1977–1999. *J. Geophys. Res.,* **108,** 3014, doi:10.1029/2001JC001044.

Munchow, A., and R. W. Garvine, 1993: Buoyancy and wind forcing of a coastal current. *J. Mar. Res.,* **51,** 293–322.

Nixon, S. W., S. Granger, B. A. Buckley, M. Lamont, and B. Rowell, 2004: A one hundred and seventeen year coastal water temperature record from Woods Hole, Massachusetts. *Estuaries,* **27,** 397–404.

Renfrew, I. A., G. W. K. Moore, P. S. Guest, and K. Bumke, 2002: A comparison of surface layer and surface turbulent flux observations over the Labrador Sea with ECMWF analyses and NCEP reanalyses. *J. Phys. Oceanogr.,* **32,** 383–400.

Rennie, S., J. L. Largier, and S. J. Lentz, 1999: Observations of low-salinity coastal current pulses downstream of Chesapeake Bay. *J. Geophys. Res.,* **104,** 18 227–18 240.

Rudnick, D. L., and R. Ferrari, 1999: Compensation of horizontal temperature and salinity gradients in the ocean mixed layer. *Science,* **283,** 526–529.

Savidge, D. K., and J. M. Bane Jr., 2001: Wind and Gulf Stream influences on along-shelf transport and off-shelf export at Cape Hatteras, North Carolina. *J. Geophys. Res.,* **106,** 11 505–11 527.

Schmitt, R. W., P. S. Bogden, and C. E. Dorman, 1989: Evaporation minus precipitation and density fluxes for the North Atlantic. *J. Phys. Oceanogr.,* **19,** 1208–1221.

Shearman, R. K., and S. J. Lentz, 2010: Long-term sea surface temperature variability along the U.S. East Coast. *J. Phys. Oceanogr.,* **40,** 1004–1017.

Stearns, F., 1965: Sea-surface temperature anomaly study of records from Atlantic coast stations. *J. Geophys. Res.,* **70,** 283–296.

Wilkin, J. L., 2006: The summertime heat budget and circulation of southeast New England shelf waters. *J. Phys. Oceanogr.,* **36,** 1997–2011.

Wright, W. R., 1976: The limits of shelf water south of Cape Cod, 1941 to 1972. *J. Mar. Res.,* **34,** 1–14.

Young, W. R., 1994: The subinertial mixed layer approximation. *J. Phys. Oceanogr.,* **24,** 1812–1826.

Yu, L., and R. A. Weller, 2007: Objectively analyzed air–sea heat fluxes for the global ice-free oceans (1981–2005). *Bull. Amer. Meteor. Soc.,* **88,** 527–539.

——, X. Jin, and R. A. Weller, 2008: Multidecade global flux datasets from Objectively Analyzed Air-Sea Fluxes (OAFlux) Project: Latent and sensible heat fluxes, ocean evaporation, and related surface meteorological variables. OAFlux Project Tech. Rep. OA-2008–01, 64 pp.